THE JOURNAL OF PHYSICAL CHEMISTRY B

Article

pubs.acs.org/JPCB

Formation of Multilayers by Star Polyelectrolytes: Effect of Number of Arms on Chain Interpenetration

Fenggui Chen,[†] Guangming Liu,*[,†] and Guangzhao Zhang[‡]

[†]Department of Chemical Physics, Hefei National Laboratory for Physical Sciences at the Microscale, University of Science and Technology of China, Hefei, P. R. China 230026

[‡]Faculty of Materials Science and Engineering, South China University of Technology, Guangzhou, P. R. China 510640

Supporting Information

ABSTRACT: We have investigated the influence of number of arms on chain interpenetration in the growth of star poly[2-(dimethylamino)ethyl methacrylate] (PDEM)/star poly(acrylic acid) (PAA) multilayers using a quartz crystal microbalance with dissipation (QCM-D). The oscillations in the changes of dissipation and frequency reflect the chain interpenetration and the variation of the mass of multilayer, respectively. The QCM-D results demonstrate that the growth of multilayers has two different mechanisms in terms of chain interpenetration. That is, the arm chains of star PDEM insert into a predeposited PAA layer to form a swollen multilayer, but the complex of star PAA with predeposited star PDEM is an "octopus-like" structure forming a dense multilayer. The transition between these two penetration modes is controlled by the number of arms in the star polyelectrolytes. As the number of arms of either PAA or PDEM increases, it becomes more difficult for star PDEM to penetrate into the PAA layer, but star PAA can more easily penetrate into the PDEM layer. According to atomic force microscopy and water contact angle measurements, all eight-bilayer multilayer surfaces have similar roughness values, and the surface wettability of the multilayers is dominated by the outermost PDEM layer.

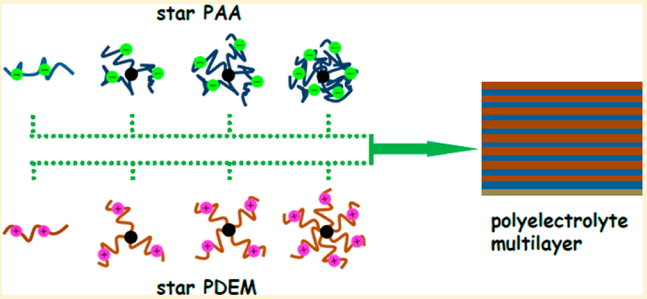

INTRODUCTION

The sequential layer-by-layer (LbL) deposition of oppositely charged polyelectrolytes on a solid substrate can generate a polyelectrolyte multilayer (PEM).[1−3] Because of the potential applications of PEMs in various fields,[4−8] the growth of PEMs has been investigated extensively.[9] In general, the formation of a PEM is influenced not only by solvent quality,[10] temperature,[11,12] pH,[13−16] ionic strength,[17,18] charge density,[19−23] and molecular weight,[24−26] but also by chain architecture.[27,28] Recent studies have shown that PEMs fabricated by star−linear or star−star polyelectrolyte pair exhibit distinct behaviors compared with their linear−linear counterpart in terms of the manner of growth or the post-treatment of multilayers.[29−33]

On the other hand, it is well-known that chain interpenetration plays a critical role in the growth of linear−linear PEMs for both linear and exponential growth modes.[34−36] In the linear growth mode, polyelectrolyte chains can interpenetrate only within the adjacent layers.[34,35] In contrast, polyelectrolyte chains can diffuse throughout the whole multilayer during exponential growth.[36] In comparison with linear−linear PEMs, multilayers formed by star polyelectrolytes usually exhibit some unique properties.[29−33] Such unique properties of star−star PEMs should be attributed to the topological structure of the star polyelectrolytes and the resulting distinct behavior of chain interpenetration between the layers. In other words, understanding the chain interpenetration behavior during multilayer growth is a prerequisite for controlling the properties of star−star PEMs. However, aside from a few studies on changes in the surface morphology of star−star PEMs,[29,31] no systematic study on chain interpenetration in star−star PEMs has been conducted to date, and the mechanism of chain interpenetration in the growth of star−star PEMs still remains unclear.

Generally, star-shaped polyelectrolytes have a more compact structure, giving rise to more limited interpenetration in comparison with that of linear chains.[29] Thus, it is expected that the behavior of chain interpenetration in the growth of star−star PEMs would be different from that in the growth of linear−linear PEMs. As the number of arms of a star polyelectrolyte changes, the resulting steric effects influence chain interpenetration.[29] In addition, the pK_a of weak polyelectrolytes changes with the number of arms because of the osmotic pressure effect,[37] leading to a corresponding change in the chain charge density and the conformations of star polyelectrolytes, which also influences the chain interpenetration. Therefore, it would be interesting to study the chain interpenetration behavior in the growth of star−star PEMs.

Received: May 23, 2012
Revised: July 23, 2012
Published: August 3, 2012

Use of a quartz crystal microbalance with dissipation (QCM-D) not only can provide information on the extent of chain interpenetration between the polyelectrolyte layers, but also can indicate which kind of polyelectrolyte will penetrate into the oppositely charged layer.[34,38,39] By use of a QCM-D, we have investigated the influences of pH, temperature, salt concentration, salt type, and chain flexibility on chain interpenetration in the growth of linear−linear PEMs.[34,38−40] Our previous studies mainly focused on how chain interpenetration is influenced by conformational changes of linear polyelectrolytes induced by variations of the external conditions. For example, we investigated how the conformational changes of linear polyelectrolytes with different chain rigidities influence multilayer growth when the external salt concentration is varied.[40] In the present work, we investigated the formation of PEMs by star poly[2-(dimethylamino)ethyl methacrylate] (PDEM) and star poly(acrylic acid) (PAA) using a QCM-D. Here, the external conditions (e.g., salt concentration and pH) were kept constant, and the polymer architecture (i.e., number of arms) was gradually changed. Our focus was on how chain interpenetration is influenced by the number of arms of star polyelectrolytes.

EXPERIMENTAL SECTION

Materials. *tert*-Butyl acrylate (*t*-BA, Aldrich) and 2-(dimethylamino)ethyl methacrylate (DEM, Aldrich, 98%) were passed through a column of alumina to remove inhibitor and then distilled over CaH_2 under reduced pressure prior to use. CuBr (AR grade) was stirred in glacial acetic acid, washed with ethanol, and then dried in a vacuum oven. Triethylamine (TEA) was stirred with KOH for 12 h at room temperature, refluxed with toluene-4-sulfonylchloride and distilled before use. *o*-Phenanthroline (AR, Sinopharm Chemical Reagent Co. Ltd., China) was recrystallized twice from hexane. Tetrahydrofuran (THF) was refluxed in the presence of sodium wire and then distilled prior to use. Acetone was refluxed in the presence of a small amount of $KMnO_4$ and then distilled from a purple sodium ketyl solution. Dichloromethane (CH_2Cl_2) was distilled under nitrogen over CaH_2. Poly(ethyleneimine) (PEI, weight-average molecular weight [M_w] ≈ 2.5 × 10^4 g mol^{-1}) was purchased from Aldrich and used as received. *N*,*N*,*N*′,*N*″,*N*″-pentamethyldiethylenetriamine (PMDETA, Aldrich), 2-bromoisobutyryl bromide (BIBB, Aldrich), and sodium azide (NaN_3, Acros) were used as received. Potassium phosphate monobasic (KH_2PO_4, 99.5%) and sodium phosphate dibasic ($Na_2HPO_4{\cdot}12H_2O$, 99%) were purchased from Sinopharm and used as received. Phosphate buffer (PB, pH ∼5.3, 0.5 M) was prepared using KH_2PO_4 and $Na_2HPO_4{\cdot}12H_2O$ and was used to prepare star polyelectrolyte solutions for LbL deposition. The water used was purified by filtration through a Millipore Gradient system after distillation, giving a resistivity of 18.2 MΩ cm.

Synthesis of Star Polyelectrolytes. Star-shaped PAA and PDEM with different numbers of arms were synthesized by atom-transfer radical polymerization (ATRP) in a core-first approach.[41,42] Details about the synthesis and characterization of the star polyelectrolytes can be found in the Supporting Information. Briefly, the difunctional initiator 1,2-bis(bromoisobutyryloxy)ethane (Br_2B) was synthesized from ethylene glycol and 2-bromoisobutyryl bromide.[43,44] The trifunctional initiator 1,1,1-trimethyolpropane tri(2-iodoisobutyrate) (Br_3T) was prepared using 1,1,1-trimethylolpropane and 2-bromoisobutyryl bromide.[45,46] The initiator with four initiating centers, pentaerythritol tetrakis(2-bromoisobutyrate) (Br_4D), was obtained by the esterification of hydroxyl group of pentaerythritol with 2-bromoisobutyryl bromide.[41,42] The initiator with six initiating centers (Br_6H) was synthesized according to the procedure reported in previous studies.[47−50] Star PDEM was directly synthesized by ATRP of DEM using multifunctional initiators. Star PAA was prepared by the hydrolysis of the star poly(*tert*-butyl acrylate) (P*t*BA), which was synthesized by ATRP of *t*-BA using multifunctional initiators. The chemical structures of star PAA and PDEM can be found in Scheme S1 (Supporting Information). The number-average molecular weight (M_n) and polydispersity index (M_w/M_n) of star PDEM were determined by gel permeation chromatography (GPC) (Waters 1515) using monodisperse polystyrene as the standard and THF as the eluent at a flow rate of 1.0 mL min^{-1}. The M_n and M_w/M_n values of star PAA were determined by GPC using monodisperse poly(ethylene glycol) as the standard and aqueous salt solution (0.1 M NaN_3, 0.01 M NaH_2PO_4) as the eluent at a flow rate of 1.0 mL min^{-1}.

QCM-D Measurements. The QCM-D and AT-cut quartz crystals were obtained from Q-sense AB.[51] The quartz crystal resonator with a fundamental resonant frequency of 5 MHz was mounted in a fluid cell with one side exposed to the solution. The resonator had a mass sensitivity constant (C) of 17.7 ng cm^{-2} Hz^{-1}. The effects of surface roughness were neglected because the resonator surfaces were highly polished with a root-mean-square (rms) roughness of less than 3 nm.[52]

When a quartz crystal is excited to oscillate in the thickness shear mode at its fundamental resonant frequency (f_0) upon application of a radio-frequency voltage across the electrodes near the resonant frequency, a small layer added to the electrodes induces a decrease in resonant frequency (Δf) that is proportional to the mass change (Δm) of the layer. In a vacuum or in air, if the added layer is rigid, evenly distributed, and much thinner than the crystal, Δf is related to Δm and the overtone number (n = 1, 3, 5, ...) by the Sauerbrey equation[53]

$$\Delta m = -\frac{\rho_q l_q}{f_0}\frac{\Delta f}{n} = -C\frac{\Delta f}{n} \quad (1)$$

where f_0 is the fundamental frequency and ρ_q and l_q are the specific density and thickness, respectively, of the quartz crystal. The dissipation factor is defined as[51]

$$D = \frac{E_d}{2\pi E_s} \quad (2)$$

where E_d is the energy dissipated during one oscillation and E_s is the energy stored in the oscillating system. The measurement of ΔD is based on the fact that the voltage over the crystal decays exponentially as a damped sinusoid when the driving power of a piezoelectric oscillator is switched off.[51] By switching the driving voltage on and off periodically, one can simultaneously obtain a series of changes of the resonant frequency and the dissipation factor.

The gold-coated resonator was cleaned using piranha solution composed of one part H_2O_2 and three parts H_2SO_4 at ∼50 °C for ∼5 min, rinsed with Milli-Q water, and blown dry with a stream of nitrogen gas. A measurement of LbL deposition was initiated by switching the liquid exposed to the resonator from water to PEI solution with a concentration of 1.0 mg mL^{-1}. PEI was allowed to adsorb onto the resonator surface for ∼20 min before the surface was rinsed with water to

dx.doi.org/10.1021/jp304994k | J. Phys. Chem. B 2012, 116, 10941−10950

ensure a uniform positively charged coating, so that the effects of the substrate on the growth of the multilayer were minimized.[10] After water was replaced with PB solution, 0.1 mg mL^{-1} PAA and PDEM were alternately introduced into the QCM cell for ~20 min with PB solution rinsing in between. Δf and ΔD values from the fundamental overtone were usually noisy because of insufficient energy trapping and were thus discarded.[54] Here, all of the values of Δf and ΔD were obtained from measurements at the third overtone (n = 3), and all experiments were conducted at 25 ± 0.02 °C. The PEI layer in the PB solution was set as the zeroth layer. The changes in frequency and dissipation induced by multilayer growth can be extracted by using each corresponding PEI layer as a reference. One can obtain information about chain interpenetration and the complexation of polyelectrolyte chains from the change of ΔD and information about the mass change of PEM from the shift of Δf.[34,39]

Atomic Force Microscopy (AFM) and Contact Angle (CA) Measurements. Polyelectrolyte multilayer-coated surfaces were imaged in air using an Nanoscope V AFM instrument (Digital Instruments, Santa Barbara, CA). The rms roughness of the multilayer surface was evaluated from the recorded AFM images. All AFM measurements were carried out in tapping mode using standard rectangular silicon cantilevers. The scanning frequency was 1.0 Hz with a resolution of 512 × 512 pixels over an area of 5 × 5 μm^2. The contact angles formed by a water droplet (~4 μL) on the multilayer surfaces were measured using a CAM 200 contact angle goniometer from KSV (Helsinki, Finland). The measurements of contact angles were performed at three different locations on the multilayer surface for each sample.

RESULTS AND DISCUSSION

In general, star-shaped polyelectrolytes can be synthesized by either the "arm-first" or "core-first" method.[41,49,55] In comparison with the arm-first method, a multifunctional initiator is used to initiate polymerization in the core-first method, giving rise to more precise control of the polyelectrolyte architecture (e.g., number of arms and arm length).[56] In the present work, star-shaped PAA and PDEM with different numbers of arms but similar arm lengths were successfully prepared using ATRP in the core-first approach (Table 1). The resulting well-defined polyelectrolyte architectures formed the basis for the subsequent studies of the influence of the number of arms on the chain interpenetration during multilayer growth. It is reported that the pK_a of weak star polyelectrolytes varies with the number of arms because of the changing osmotic pressure inside the star polymers.[31] Here, the pK_a increased from ~4.5 for linear PAA to ~5.4 for six-arm star PAA,[57,58] whereas the pK_a decreased from ~6.5 for linear PDEM to ~6.0 for six-arm star PDEM.[29,59] Because all of the polymer solutions were prepared using PB with a pH of ~5.3, PAA gradually changed from an almost completely charged state to a ~50% charged state as the number of arms increased from two to six, and the charge density of PDEM remained almost constant as the number of arms increased from two to six.

Table 1. Molecular Characteristics of Star PAA and PDEM

no.	polymer	M_n[a] (g mol^{-1})	n_{arm}[b]	M_w/M_n[a]
1	two-arm PAA	5.9×10^3	38	1.06
2	three-arm PAA	8.3×10^3	36	1.06
3	four-arm PAA	1.1×10^4	34	1.04
4	six-arm PAA	1.3×10^4	28	1.07
5	two-arm PDEM	1.8×10^4	56	1.28
6	three-arm PDEM	2.3×10^4	47	1.29
7	four-arm PDEM	3.0×10^4	46	1.28
8	six-arm PDEM	4.6×10^4	47	1.27

[a] M_n and M_w/M_n for star PAA were determined by GPC using monodisperse poly(ethylene glycol) as the standard and salt solution (0.1 M NaN_3, 0.01 M NaH_2PO_4) as the eluent. M_n and M_w/M_n for star PDEM were determined by GPC using monodisperse polystyrene as the standard and THF as the eluent. [b] Average number of monomers in each arm of the star polyelectrolytes.

Figure 1 shows the shifts in ΔD and $-\Delta f$ as a function of number of layers for the different PAA–PDEM pairs, where the odd and even numbers of layers correspond to the deposition of PAA and PDEM, respectively. The number combinations (e.g., 2–2) in the figure legend represent the different PAA–PDEM pairs. The first and second numbers denote the number of arms of star PAA and star PDEM, respectively. For Figure 1, the number of arms of PAA was fixed at two (linear chain), and the number of arms of PDEM was gradually increased from two to six. It is known that the dissipation factor of a film relates to its structure.[34,38] A dense and rigid layer has a small dissipation factor, whereas a swollen and loose layer has a large one.[60] In the case of the 2–2 pair, ΔD increased in an oscillatory manner with the number of layers, indicating the alternating deposition of PAA and PDEM on the QCM chip surface. Our previous studies demonstrated that the oscillation in the changes of ΔD is an indication of chain interpenetration.[34,38] Here, the increase in ΔD for odd numbers of layers indicates that the deposited PAA chains form a swollen layer on the surface, whereas the decrease in ΔD for even numbers of layers implies that the adsorbed PDEM chains penetrate into the predeposited PAA layer and form a relatively dense layer through polyelectrolyte complexation. Such complexation could extend a certain depth into the layer; that is, chain interpenetration between PAA and PDEM layers occurred. After the adsorption of PDEM, the surface charge changed

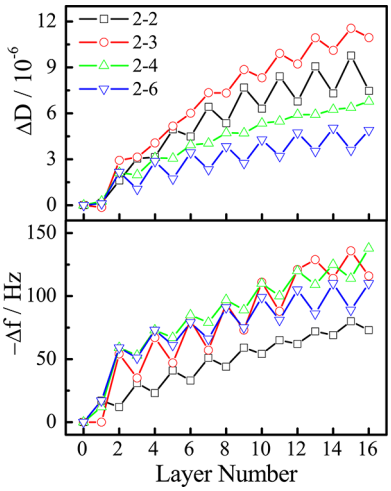

Figure 1. Shifts in dissipation (ΔD) and frequency ($-\Delta f$) as a function of number of layers for the different PAA–PDEM pairs, where the odd and even numbers of layers correspond to the deposition of PAA and PDEM, respectively, and the number of arms of PAA is fixed at 2 for all the pairs.

dx.doi.org/10.1021/jp304994k | J. Phys. Chem. B 2012, 116, 10941–10950

from negative to positive, making the subsequent adsorption of PAA possible. Consequently, the oscillating changes in ΔD with the number of layers indicate the alternating swelling and shrinking of the outermost layer of the multilayer due to the chain interpenetration. Obviously, in the case of the 2−2 pair, the PDEM chains penetrate into the PAA layer. Likewise, in the case of the 2−3 pair, the arm chains of PDEM also penetrate into the PAA layer, as reflected by the fact that ΔD increases and decreases for odd and even numbers of layers, respectively.

However, no obvious oscillations in ΔD with the number of layers were observed for the 2−4 pair, indicating that only slight chain interpenetration occurred in this case. This is understandable because the more prominent steric effect created by star PDEM prevents chain interpenetration as the number of arms increases to four. When the number of arms is increased to six, the steric effect created by star PDEM should be more notable.[61] Nonetheless, chain interpenetration was observed again in the case of the 2−6 pair. More interestingly, the increase in ΔD for the even numbers of layers and the decrease in ΔD for the odd numbers of layers imply that the PAA chains penetrated into the PDEM layer, which is in contrast to the behavior for the 2−2 and 2−3 pairs. From this discussion, one can conclude that it is more difficult for star PDEM to penetrate into the PAA layer as the number of arms of PDEM increases because of the increasing steric effect. Moreover, the value of ΔD for the 2−6 pair is much smaller than that for the 2−2 and 2−3 pairs for the same number of layers, indicating that the mechanism of chain interpenetration or complexation in the former case might be different from that in the latter cases. We will return to this point later. Clearly, the 2−4 pair is a critical case at which the behavior of chain interpenetration changes dramatically; specifically, the arm chains of PDEM penetrate into the PAA layer when the number of arms of PDEM is less than four, whereas the PAA chains penetrate into the PDEM layer when the number of arms of PDEM is greater than four.

On the other hand, the gradual increases of $-\Delta f$ with the number of layers indicate the sequential deposition of polyelectrolytes on the surface. Basically, $-\Delta f$ relates to the mass change of the PEM, which is determined by the competition between the adsorption of polyelectrolyte chains and the release of trapped water molecules from the PEM during polyelectrolyte complexation.[34] In the cases of 2−2 and 2−3 pairs, $-\Delta f$ increases for the odd numbers of layers, indicating an increase of the mass of the PEM induced by the adsorption of PAA chains, and the decrease of $-\Delta f$ for the even numbers of layers indicates a decrease of the mass of the PEM due to the release of trapped water molecules during the penetration of PDEM arm chains into the PAA layer. In other words, the mass changes of PEM for odd and even numbers of layers are dominated by the adsorption of PAA chains and the release of trapped water molecules, respectively. Clearly, the oscillations in the changes of $-\Delta f$ imply the alternating increase and decrease of the mass of the PEM during LbL deposition. In the case of the 2−6 pair, the increase of $-\Delta f$ for even numbers of layers indicates an increase of the mass of the PEM because of the deposition of PDEM, and the decrease of $-\Delta f$ for the odd numbers of layers implies a decrease of the mass of the PEM due to the release of trapped water molecules during the penetration of PAA chains into the PDEM layer. In the case of the 2−4 pair, the small oscillations of $-\Delta f$ with the number of layers might suggest small oscillating changes in the mass of the PEM during the interfacial complexation between PAA and PDEM. Obviously, the results obtained from the changes of $-\Delta f$ are consistent with those obtained from the changes of ΔD.

The steric barrier created by three-arm star PAA is larger than that created by two-arm PAA. Therefore, it is expected that it will be more difficult for PDEM to penetrate into the layer formed by the three-arm PAA. Figure 2 shows the shifts in

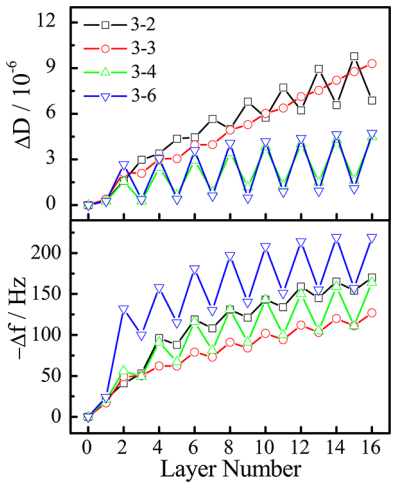

Figure 2. Shifts in dissipation (ΔD) and frequency ($-\Delta f$) as a function of number of layers for different PAA−PDEM pairs, where the odd and even numbers of layers correspond to the deposition of PAA and PDEM, respectively, and the number of arms of PAA is fixed at 3 for all pairs.

ΔD and $-\Delta f$ as a function of number of layers for the different PAA−PDEM pairs, where the number of arms of PAA is fixed at three for all of the pairs. In the case of the 3−2 pair, the increase in ΔD for the odd numbers of layers and the decrease in ΔD for the even numbers of layers indicate the penetration of PDEM arm chains into the PAA layer, which is similar to the cases for the 2−2 and 2−3 pairs. However, when the number of arms of PDEM increased to three, no obvious oscillations in the change of ΔD with the number of layers were observed, implying that only interfacial polyelectrolyte complexation occurred for the 3−3 pair, which might merely lead to slight chain interpenetration between the PAA and PDEM layers. For the 3−4 and 3−6 pairs, ΔD increased for the even numbers of layers but decreased for the odd numbers of layers, suggesting the penetration of PAA arm chains into the PDEM layer. Clearly, as the number of arms of PAA increased from two to three, the number of arms of PDEM required to allow chain interpenetration from the PDEM- to the PAA-dominated regime decreased from four to three. This fact indicates that it is more difficult for PDEM to penetrate into the PAA layer as the number of arms of PAA increases because of the increasing steric effect created by star PAA. Again, the values of ΔD in the cases of the 3−4 and 3−6 pairs were smaller than that in the case of the 3−2 pair for the same number of layers, implying that the mechanism of chain interpenetration in the PDEM-dominated regime might be different from that in the PAA-dominated regime.

On the other hand, in the case of the 3−2 pair, the oscillations in the change of $-\Delta f$ with the number of layers imply an oscillating mass change of the PEM due to the competition between the adsorption of polyelectrolyte chains and the release of trapped water molecules. For the 3−3 pair,

dx.doi.org/10.1021/jp304994k | J. Phys. Chem. B 2012, 116, 10941−10950

$-\Delta f$ exhibits small oscillations with the number of layers, indicating a slightly oscillating change in the mass of the PEM during interfacial polyelectrolyte complexation. In the cases of the 3−4 and 3−6 pairs, the increase in $-\Delta f$ for the even numbers of layers indicates an increase in the mass of the PEM due to the adsorption of star PDEM, and the decrease of $-\Delta f$ for the odd numbers of layers implies a decrease in the mass of the PEM due to the release of trapped water molecules during the penetration of PAA arm chains into the PDEM layer.

Figure 3 shows the shifts in ΔD and $-\Delta f$ as a function of the number of layers for different PAA−PDEM pairs, where the

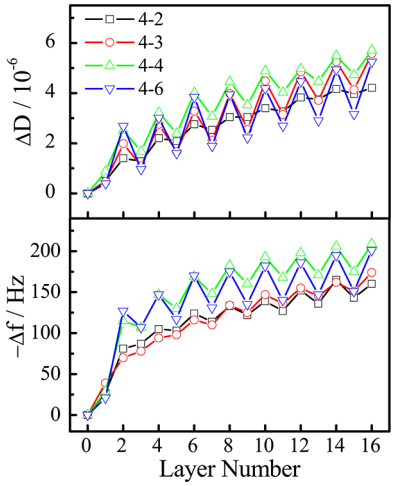

Figure 3. Shifts in dissipation (ΔD) and frequency ($-\Delta f$) as a function of number of layers for different PAA−PDEM pairs, where the odd and even numbers of layers correspond to the deposition of PAA and PDEM, respectively, and the number of arms of PAA is fixed at 4 for all pairs.

number of arms of PAA is fixed at four for all of the pairs. In the case of the 4−2 pair, no obvious oscillations were observed in the change of ΔD with the number of layers, suggesting that only slight chain interpenetration occurs in this case. For all of the residual pairs, ΔD increased for the even numbers of layers but decreased for the odd numbers of layers, indicating that the PAA arm chains penetrated into the PDEM layer. In other words, no PDEM-dominated penetration regime was observed when the number of arms of PAA increased to four. This is because the large steric barrier created by star PAA prevents the penetration of PDEM into the PAA layer even for two-arm PDEM. On the other hand, the small oscillations in the change of $-\Delta f$ with the number of layers for the 4−2 pair suggests the slightly oscillating change in the mass of the PEM during interfacial polyelectrolyte complexation. For the 4−3, 4−4, and 4−6 pairs, the increase in $-\Delta f$ for even numbers of layers indicates an increase of the mass of the PEM due to the adsorption of star PDEM, and the decrease of $-\Delta f$ for odd numbers of layers implies a decrease of the mass of the PEM due to the release of trapped water molecules during the penetration of star PAA.

It is expected that the steric effect created by star PAA becomes more obvious when the number of arms of PAA increases to six; thus, it is more difficult for PDEM to penetrate into the PAA layer. Figure 4 shows that ΔD increased for even numbers of layers but decreased for odd numbers of layers for all pairs with the number of arms of PAA fixed at six, indicating that PAA arm chains penetrate into the PDEM layer regardless

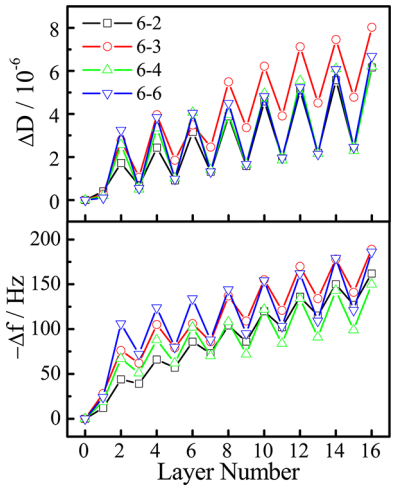

Figure 4. Shifts in dissipation (ΔD) and frequency ($-\Delta f$) as a function of number of layers for different PAA−PDEM pairs, where the odd and even numbers of layers correspond to the deposition of PAA and PDEM, respectively, and the number of arms of PAA is fixed at 6 for all pairs.

of the number of arms of PDEM. On the other hand, the mass change of the PEM was dominated by the adsorption of polyelectrolyte and the release of trapped water molecules for the deposition of PDEM and PAA, respectively, as indicated by the fact that $-\Delta f$ increased for even numbers of layers but decreased for odd numbers of layers. From Figures 1−4, it can be concluded that it is more difficult for star PDEM to penetrate into the PAA layer as the number of arms of either PDEM or PAA increases because of the increasing steric effect.

To understand how the number of arms of star PAA influences chain interpenetration, we investigated the changes in ΔD and $-\Delta f$ with the number of layers when the number of arms of PDEM was fixed and the number of arms of PAA was varied. Figure 5 shows the shifts in ΔD and $-\Delta f$ as a function of number of layers for different PAA−PDEM pairs, where the number of arms of PDEM was fixed at two for all of the pairs.

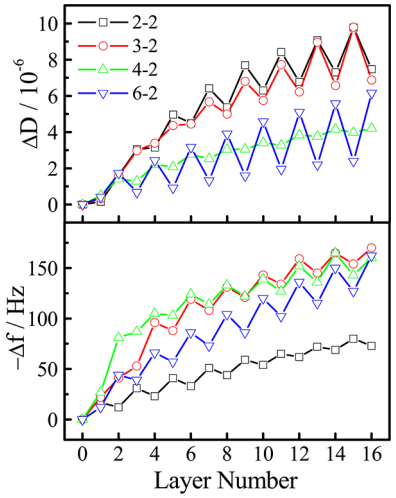

Figure 5. Shifts in dissipation (ΔD) and frequency ($-\Delta f$) as a function of number of layers for different PAA−PDEM pairs, where the odd and even numbers of layers correspond to the deposition of PAA and PDEM, respectively, and the number of arms of PDEM is fixed at 2 for all pairs.

dx.doi.org/10.1021/jp304994k | J. Phys. Chem. B 2012, 116, 10941−10950

For the 2−2 and 3−2 pairs, the increase in ΔD for odd numbers of layers and the decrease in ΔD for even numbers of layers indicate the penetration of the PDEM arm chains into the PAA layer. As the number of arms of PAA increased to four, only slight chain interpenetration occurred during LbL deposition, as indicated by the fact that no obvious oscillations were observed in the change of ΔD with the number of layers. In the case of the 6−2 pair, the increase in ΔD for even numbers of layers and the decrease in ΔD for odd numbers of layers imply the penetration of the PAA arm chains into the PDEM layer. Clearly, as the number of arms of PAA increased, star PAA could more easily penetrate into the PDEM layer, which is quite different from the behavior in the PDEM-dominated penetration regime. In addition, the value of ΔD in the case of the 6−2 pair was smaller than those in the cases of the 2−2 and 3−2 pairs for the same number of layers, further suggesting different mechanisms of chain interpenetration between the PAA- and PDEM-dominated penetration regimes. On the other hand, the oscillations in the changes of $-\Delta f$ with the number of layers for the 2−2, 3−2, 4−2, and 6−2 pairs are indicative of the oscillating variations in the mass of the PEM during multilayer growth.

Figure 6 shows the shifts in ΔD and $-\Delta f$ as a function of number of layers for different PAA−PDEM pairs, where the

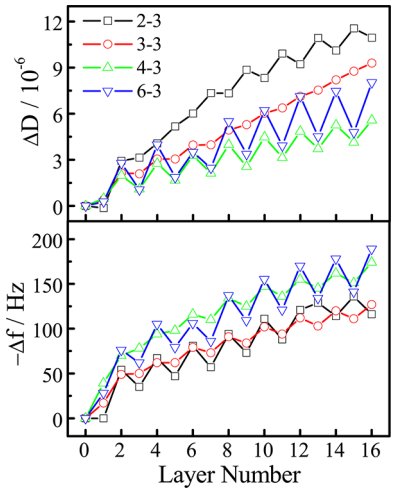

Figure 6. Shifts in dissipation (ΔD) and frequency ($-\Delta f$) as a function of number of layers for different PAA−PDEM pairs, where the odd and even numbers of layers correspond to the deposition of PAA and PDEM, respectively, and the number of arms of PDEM is fixed at 3 for all pairs.

number of arms of PDEM was fixed at three for all of the pairs. It can be seen that ΔD increased and decreased for odd and even numbers of layers, respectively, in the case of the 2−3 pair, indicating that chain interpenetration was dominated by the penetration of PDEM. For the 4−3 and 6−3 pairs, the increase in ΔD for even numbers of layers and the decrease in ΔD for odd numbers of layers suggest that chain interpenetration in the two cases is dominated by the penetration of PAA. In the case of the 3−3 pair, only slight chain interpenetration occurred, as reflected by the fact that no obvious oscillations were observed in the change of ΔD with the number of layers. Clearly, as the number of arms of PDEM increased from two to three, the number of arms of PAA required to allow chain interpenetration from the PDEM- to the PAA-dominated regime decreased from four to three. That is, star PAA can more easily penetrate into the PDEM layer with increasing number of arms of PDEM. Additionally, the values of ΔD in the PAA-dominated penetration regime are smaller than those in the PDEM-dominated penetration regime for the same number of layers, which is similar to that in Figure 5. Moreover, the oscillations in the changes of $-\Delta f$ with the number of layers for the 2−3, 3−3, 4−3, and 6−3 pairs indicate oscillating variations in the mass of the PEM during multilayer growth.

In Figure 7, for the 2−4 pair, no obvious oscillations in ΔD with the number of layers were observed, implying that only

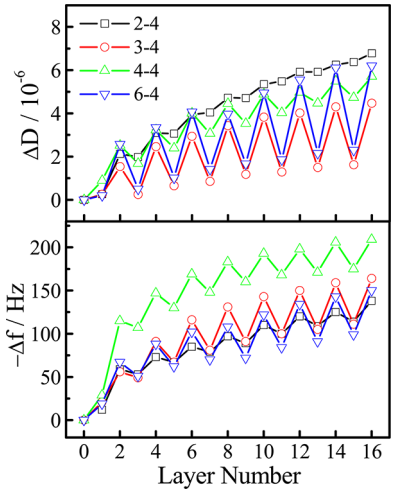

Figure 7. Shifts in dissipation (ΔD) and frequency ($-\Delta f$) as a function of number of layers for different PAA−PDEM pairs, where the odd and even numbers of layers correspond to the deposition of PAA and PDEM, respectively, and the number of arms of PDEM is fixed at 4 for all pairs.

slight chain interpenetration occurred in this case. For the 3−4, 4−4, and 6−4 pairs, ΔD increased and decreased for even and odd numbers of layers, respectively, indicating that chain interpenetration was dominated by the penetration of PAA. Again, the oscillations in the changes of $-\Delta f$ with the number of layers for the 2−4, 3−4, 4−4, and 6−4 pairs indicate oscillating variations in the mass of the PEM during LbL deposition. Likewise, as the number of arms of PDEM increased to six (Figure 8), ΔD increased for even numbers of layers but decreased for odd numbers of layers for all of the pairs, implying that chain interpenetration was dominated by the penetration of PAA. The oscillations of $-\Delta f$ with the number of layers for the 2−6, 3−6, 4−6, and 6−6 pairs are the indicative of the oscillating changes of the mass of the PEM during the multilayer growth. From Figures 5−8, it can be concluded that star PAA can more easily penetrate into the PDEM layer as the number of arms of either PAA or PDEM increases.

On the basis of Figures 1−8, one can conclude that the mechanism of chain interpenetration in the PDEM-dominated penetration regime is different from that in the PAA-dominated penetration regime. More specifically, as the number of arms of either PAA or PDEM increases, it is more difficult for star PDEM to penetrate into the PAA layer, but star PAA can more easily penetrate into the PDEM layer. Note that chain interpenetration can only occur within adjacent layers because all of the multilayers are formed in a linear manner.[34−36] The arm chains of the PDEM retain a completely charged state as the number of arms increases from two to six, whereas the

dx.doi.org/10.1021/jp304994k | J. Phys. Chem. B 2012, 116, 10941−10950

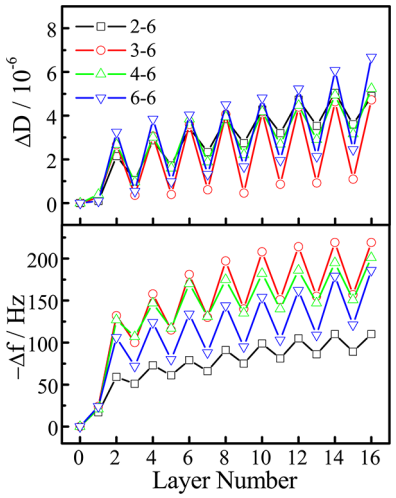

Figure 8. Shifts in dissipation (ΔD) and frequency ($-\Delta f$) as a function of number of layers for different PAA–PDEM pairs, where the odd and even numbers of layers correspond to the deposition of PAA and PDEM, respectively, and the number of arms of PDEM is fixed at 6 for all pairs.

charge fraction of the arm chains of PAA gradually decreases from ~100% to ~50% as the number of arms increases from two to six.[58] In the present work, all experiments were conducted at a NaCl concentration of 0.5 M; thus, the Debye length was ~0.4 nm, so that the long-range electrostatic interactions were screened and the conformation of the star polyelectrolytes was not strongly dependent on the charge state of the arm chains. Nevertheless, the conformation could still be influenced by the charge fraction of the arm chains (see below).

Generally, the conformation of the polyelectrolytes is determined by the total chain persistence length (l_p), which represents the effective rigidity of the polyelectrolyte chain.[62] l_p is the sum of the intrinsic persistence length (l_0) and the electrostatic persistence length (l_e)[63]

$$l_p = l_0 + l_e = l_0 + \frac{l_B \tau^2}{4\kappa^2}$$

where l_B, τ, and κ^{-1} are the Bjerrum length, the linear charge density, and the Debye length, respectively. τ is defined as $\tau = f/b$, where f is the charge fraction of polymer chain and b is the bond length. l_0 for PDEM and PAA is ~0.9 and ~0.7 nm, respectively.[64,65] At a NaCl concentration of 0.5 M and a pH of 5.3, the l_p value of star PDEM is ~2.1 nm irrespective of the number of arms because the charge fraction is ~100% for all star PDEM. For star PAA at the same conditions, l_p decreases from ~1.9 nm for two-arm PAA to ~1.0 nm for six-arm PAA because the charge fraction decreases from ~100% to ~50% as the number of arms increases from two to six. That is, the arm chains can adopt a more coiled conformation as the number of arms of PAA increases. Detailed calculations can be found in the Supporting Information.

It is known that polyelectrolyte chains with a relatively long persistence length can insert into a layer formed by oppositely charged chains with a shorter persistence length.[39] Thus, PDEM with a low number of arms would insert into the predeposited PAA layer, and this penetration would become more difficult and be hindered by the steric barrier as the number of arms of either PAA or PDEM increases (Scheme 1). This is why it is more difficult for star PDEM to penetrate into the PAA layer with increasing number of arms of PDEM or PAA. On the other hand, the arm chains adopt a more coiled conformation with increasing number of arms of PAA.

Scheme 1. Mechanisms for Chain Interpenetration in the Growth of Star PAA/Star PDEM Multilayers[a]

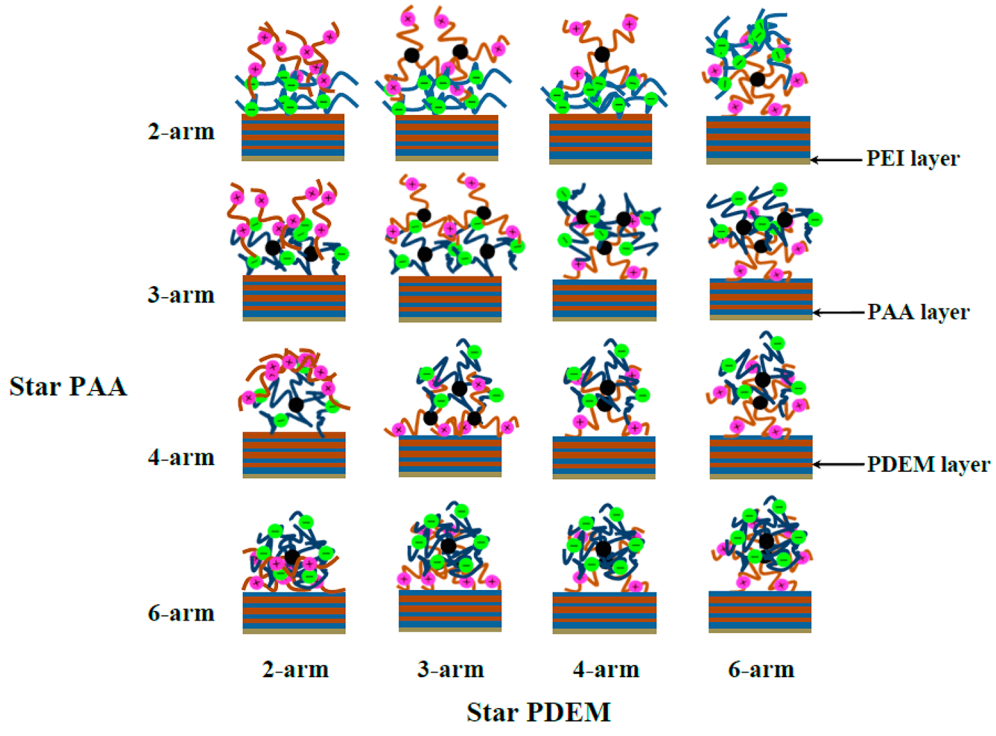

[a]Outermost bilayer deliberately magnified compared with other layers, so that chain interpenetration can be seen more clearly.

dx.doi.org/10.1021/jp304994k | J. Phys. Chem. B 2012, 116, 10941–10950

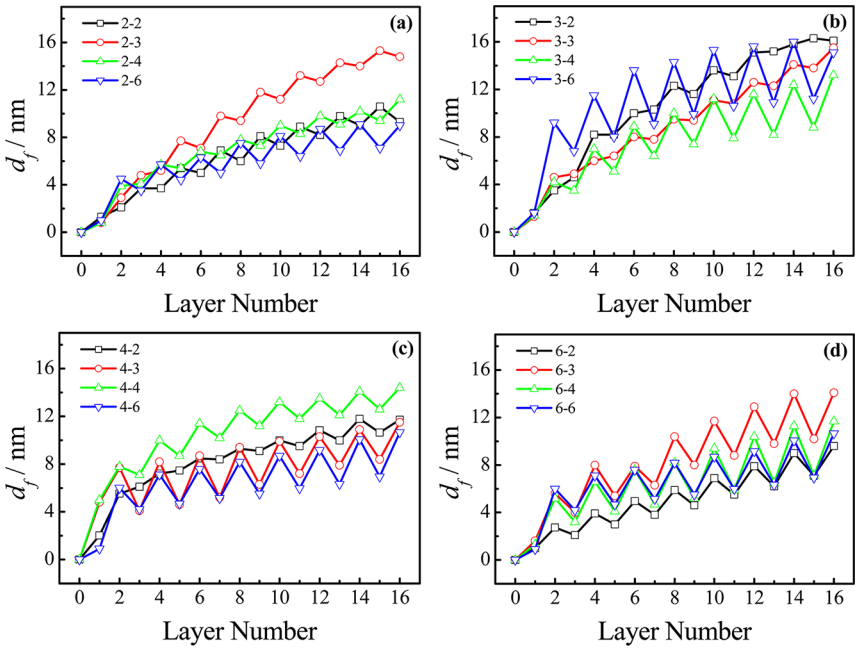

Figure 9. Changes in the hydrodynamic thickness (d_f) of PEM as a function of number of layers for all PAA–PDEM pairs fit by the Voigt model based on the shifts of Δf and ΔD at different overtones, where the odd and even numbers of layers correspond to the deposition of PAA and PDEM, respectively. Number of arms of PAA fixed at (a) 2, (b) 3, (c) 4, and (d) 6.

Therefore, it is expected that the penetration of PAA into the PDEM layer might occur in a different manner, that is, star PAA can complex with the predeposited PDEM layer in an "octopus-like" structure (Scheme 1). Increasing number of arms of PAA lead to a more coiled conformation of the arm chains and result in more effective complexation between PAA and PDEM. Moreover, increasing number of arms of PDEM would provide more complexation sites during the penetration of PAA. Thus, more arm chains in star PAA or PDEM will be more favorable for polyelectrolyte complexation. This is why star PAA can more easily penetrate into the PDEM layer with increasing number of arms of PAA or PDEM. Furthermore, the PEM would have a swollen structure in the PDEM-dominated penetration regime due to the relatively extended conformation of star PDEM, whereas star PAA and PDEM would form a relatively dense PEM structure in the PAA-dominated penetration regime because of the effective complexation between polyelectrolyte chains. This is why the ΔD value in the PAA-dominated penetration regime is always lower than that in the PDEM-dominated penetration regime for the same number of layers (Figures 1, 2, 5, and 6).

Now, one can understand why there is a critical case at which the behavior of chain interpenetration changes dramatically. See Figure 1 as an example, for the 2–2 and 2–3 pairs, where PDEM penetrates into the predeposited PAA layer, as reflected by the fact that ΔD increases and decreases for odd and even numbers of layers, respectively. In the case of 2–4 pair, no obvious oscillations can be observed in the change of ΔD with the number of layers, indicating that only interfacial polyelectrolyte complexation between PAA and PDEM occurs in this case. Clearly, as the number of arms of PDEM increases from two to four, the steric effect produced by the PDEM becomes more prominent, so that the large steric barrier created by four-arm PDEM prevents the penetration of PDEM into the PAA layer. When the number of arms of PDEM is increased to six, the steric effect created by PDEM should be more marked, and it should be more difficult for PDEM to penetrate into the PAA layer. However, chain interpenetration is observed again in the case of 2–6 pair, as indicated by the oscillations in the change of ΔD. One should be aware that PAA can penetrate into the PDEM layer in this case as reflected by the increase in ΔD for even numbers of layers and the decrease in ΔD for odd numbers of layers, which is in contrast to the cases of 2–2 and 2–3 pairs. This is because six-arm PDEM with a number of complexation sites favors the penetration of PAA into the predeposited PDEM layer by polyelectrolyte complexation. For four-arm PDEM, the steric barrier created by PDEM prevents the insertion of the arm chains of PDEM into the PAA layer. Meanwhile, the complexation sites on the four-arm PDEM might not be strong enough to induce the effective penetration of two-arm PAA into the PDEM layer by polyelectrolyte complexation. That is, only interfacial polyelectrolyte complexation occurs in the case of 2–4 pair. This is why the 2–4 pair is the critical point and four-arm PDEM is so special in Figure 1. Actually, the critical pair varies with the number of arms of PAA. For the two-arm, three-arm, and four-arm PAAs, the critical pairs are 2–4, 3–3, and 4–2, respectively (Figures 1–3), indicating that it is more difficult for PDEM to penetrate into the PAA layer with increasing number of arms of PAA.

Figure 9 shows the changes in the hydrodynamic thickness (d_f) of the PEM as a function of the number of layers for all of the PAA–PDEM pairs fit by the Voigt model based on the shifts in Δf and ΔD at different overtones. The oscillating changes in d_f with number of layers indicate the alternating swelling and shrinking of the outermost layer induced by chain interpenetration. Specifically, the increase in d_f is indicative of the formation of a swollen outermost layer by adsorbed polyelectrolytes, and the decrease in d_f indicates the shrinking of the outermost layer due to polyelectrolyte complexation during chain interpenetration. In Figure 9a, d_f increases for odd numbers of layers but decreases for even numbers of layers for

dx.doi.org/10.1021/jp304994k | J. Phys. Chem. B 2012, 116, 10941–10950

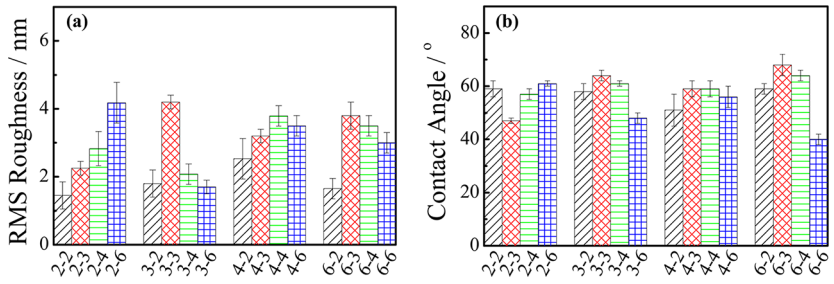

Figure 10. (a) rms roughness and (b) static contact angles for the eight-bilayer PEM surfaces for all pairs.

the 2−2 and 2−3 pairs, indicating that chain interpenetration is dominated by the penetration of PDEM in these two cases. In the case of the 2−6 pair, the increase in d_f for even numbers of layers and the decrease in d_f for odd numbers of layers imply that chain interpenetration is dominated by the penetration of PAA. In Figure 9b, the small oscillations in the change of d_f for the 3−2 pair could suggest a relatively low extent of the chain interpenetration. For the 3−4 and 3−6 pairs, d_f decreases and increases for odd and even numbers of layers, respectively, indicating the penetration of star PAA into the PDEM layer. In Figure 9c,d, d_f decreases for odd numbers of layers but increases for even numbers of layers for all pairs, with the exception of the 4−2 pair, implying that chain interpenetration is dominated by the penetration of PAA. For the 2−4, 3−3, and 4−2 pairs, no obvious oscillations are observed in the changes of d_f with the number of layers, implying that only slight chain interpenetration occurs for these pairs.

The rms roughness and static contact angles for eight-bilayer PEM surfaces are shown in Figure 10. The rms roughness for all of the pairs is ∼3 nm (Figure 10a), suggesting that all the PEM surfaces have a similar roughness regardless of the polyelectrolyte architectures. It is known that surface wettability is influenced not only by the surface chemical component but also by the surface roughness.[66] Because all of the PEM surfaces have similar roughness values, the surface wettability of the multilayers should be governed by the surface chemical component. Figure 10b shows that the static contact angles of the PEM surfaces are located around ∼60°, implying that all of the PEM surfaces have similar wettabilities. The wettabilities of the PAA- and PDEM-coated surfaces were also checked, and the static contact angles of the PAA- and PDEM-coated surfaces were found to be ∼29° and ∼63°, respectively. These facts indicate that the wettability of the PEM surfaces is dominated by the outermost PDEM layer, even though the expected interpenetration of PAA arm chains across the PAA/PDEM interface could give rise to a slight decrease of the contact angles.

CONCLUSIONS

In the present work, we have investigated the influence of the number of arms on the chain interpenetration in the formation of PEMs by star PAA and star PDEM. The growth of multilayers exhibits two different mechanisms in terms of chain interpenetration. The insertion of PDEM with a low number of arms into a predeposited PAA layer would result in a swollen multilayer. In contrast, star PAA can effectively complex with the predeposited PDEM layer in an octopus-like structure, leading to a relatively dense multilayer. Moreover, as the number of arms of either PDEM or PAA increases, it is more difficult for star PDEM to penetrate into the PAA layer, whereas star PAA can more easily penetrate into the PDEM layer. In addition, the wettability of the PEM surfaces is dominated by the outermost PDEM layer.

ASSOCIATED CONTENT

Supporting Information

Details on the synthesis and characterization of star PAA and PDEM and calculation of the chain persistence length. This material is available free of charge via the Internet at http://pubs.acs.org.

AUTHOR INFORMATION

Corresponding Author

*E-mail: gml@ustc.edu.cn.

Notes

The authors declare no competing financial interest.

ACKNOWLEDGMENTS

Financial support from the National Program on Key Basic Research Project (2012CB933802), the National Natural Science Foundation of China (21004058, 91127042), the Scientific Research Startup Foundation of the Chinese Academy of Sciences, and the Fundamental Research Funds for the Central Universities (WK2060030008) is acknowledged.

REFERENCES

(1) Ariga, K.; Lvov, Y.; Kunitake, T. *J. Am. Chem. Soc.* **1997**, *119*, 2224−2231.
(2) Tsukruk, V. V.; Bliznyuk, V. N.; Visser, D.; Campbell, A. L.; Bunning, T. J.; Adams, W. W. *Macromolecules* **1997**, *30*, 6615−6625.
(3) Lowack, K.; Helm, C. A. *Macromolecules* **1998**, *31*, 823−833.
(4) Eckle, M.; Decher, G. *Nano Lett.* **2001**, *1*, 45−49.
(5) Hiller, J.; Mendelsohn, J. D.; Rubner, M. F. *Nat. Mater.* **2002**, 59−63.
(6) Ram, M. K.; Carrara, S.; Paddeu, S.; Nicolini, C. *Thin Solid Films* **1997**, *302*, 89−97.
(7) Laschewsky, A.; Mayer, B.; Wischerhoff, E.; Arys, X.; Bertrand, P.; Delcorte, A.; Jonas, A. *Thin Solid Films* **1996**, *284−285*, 334−337.
(8) Lzumrudov, V. A.; Kharlampieva, E.; Sukhishvili, S. A. *Biomacromolecules* **2005**, *6*, 1782−1788.
(9) Yuri, L.; Michael, M. In *Dekker Encyclopedia of Nanoscience and Nanotechnology*, 2nd ed.; CRC Press: Boca Raton, FL, 2008; pp 1823−1840.
(10) Poptoshev, E.; Schoeler, B.; Caruso, F. *Langmuir* **2004**, *20*, 829−834.
(11) Ma, J. H.; Yang, S. G.; Li, Y. F.; Xu, X.; Xu, J. *Soft Matter* **2011**, *7*, 9435−9443.
(12) Greinert, N.; Richtering, W. *Colloid Polym. Sci.* **2004**, *282*, 1146−1149.
(13) Kharlampieva, E.; Sukhishvili, S. A. *Langmuir* **2003**, *19*, 1235−1243.
(14) Mauser, T.; Dejugnat, C.; Sukhorukov, G. B. *Macromol. Rapid Commun.* **2004**, *25*, 1781−1785.

(15) Lulevich, V. V.; Vinogradova, O. I. *Langmuir* **2004**, *20*, 2874−2878.
(16) Yang, S. G.; Zhang, Y. J.; Zhang, X. L.; Xu, J. *Soft Matter* **2007**, *3*, 463−469.
(17) Dodoo, S.; Steitz, R.; Laschewsky, A.; von Klitzing, R. *Phys. Chem. Chem. Phys.* **2011**, *13*, 10318−10325.
(18) Boddohi, S.; Killingsworth, C. E.; Kipper, M. J. *Biomacromolecules* **2008**, *9*, 2021−2028.
(19) Glinel, K.; Moussa, A.; Jonas, A. M.; Laschewsky, A. *Langmuir* **2002**, *18*, 1408−1412.
(20) Koetse, M.; Laschewsky, A.; Jonas, A. M.; Wagenknecht, W. *Langmuir* **2002**, *18*, 1655−1660.
(21) Schoeler, B.; Kumaraswamy, G.; Caruso, F. *Macromolecules* **2002**, *35*, 889−897.
(22) Voigt, U.; Khrenov, V.; Thuer, K.; Hahn, M.; Jaeger, W.; von Klitzing, R. *J. Phys.: Condens. Mater.* **2003**, *15*, 213−218.
(23) Choi, J.; Rubner, M. F. *Macromolecules* **2005**, *38*, 116−124.
(24) Das, S.; Pal, A. J. *Langmuir* **2002**, *18*, 458−461.
(25) Sui, Z. J.; Salloum, D.; Schlenoff, J. B. *Langmuir* **2003**, *19*, 2491−2495.
(26) Houska, M.; Brynda, E.; Bohatá, K. *J. Colloid Interface Sci.* **2004**, *273*, 140−147.
(27) Zhou, L.; Yan, L. Y.; Xue, J.; Chen, L.; Wang, Y. P.; Jia, Z. F.; Zhu, X. Y.; Yan, D. Y. *J. Appl. Polym. Sci.* **2007**, *104*, 2323−2329.
(28) Larin, S. V.; Darinskii, A. A.; Zhulina, E. B.; Borisov, O. V. *Langmuir* **2009**, *25*, 1915−1918.
(29) Choi, I.; Suntivich, R.; Plamper, F. A.; Synatschke, C. V.; Müller, A. H. E.; Tsukruk, V. V. *J. Am. Chem. Soc.* **2011**, *133*, 9592−9606..
(30) Guo, Z. Z.; Chen, X. Y.; Xin, J. Y.; Wu, D.; Li, J. S.; Xu, C. L. *Macromolecules* **2010**, *43*, 9087−9093.
(31) Kim, B. S.; Gao, H.; Argun, A. A.; Matyjaszewski, K.; Hammond, P. T. *Macromolecules* **2009**, *42*, 368−375.
(32) Pergushov, D. V.; Babin, I. A.; Plamper, F. A.; Zezin, A. B.; Müller, A. H. E. *Langmuir* **2008**, *24*,, 6414−6419..
(33) Connal, L. A.; Li, Q.; Quinn, J. F.; Tjipto, E.; Caruso, F.; Qiao, G. G. *Macromolecules* **2008**, *41*, 2620−2626.
(34) Liu, G. M.; Zhao, J. P.; Sun, Q. Y.; Zhang, G. Z. *J. Phys. Chem. B* **2008**, *112*, 3333−3338.
(35) Salomäki, M.; Vinokurov, I. A.; Kankare, J. *Langmuir* **2005**, *21*, 11232−11240.
(36) Porcel, C.; Lavalle, P.; Ball, V.; Decher, G.; Senger, B.; Voegel, J. C.; Schaaf, P. *Langmuir* **2006**, *22*, 4376−4383.
(37) Plamper, F. A.; Becker, H.; Lanzendörfer, M.; Patel, M.; Wittemann, A.; Ballauff, M.; Müller, A. H. E. *Macromol. Chem. Phys.* **2005**, *206*, 1813−1825.
(38) Liu, G. M.; Zou, S. R.; Fu, L.; Zhang, G. Z. *J. Phys. Chem. B* **2008**, *112*, 4167−4171.
(39) Liu, G. M.; Hou, Y.; Xiao, X.; Zhang, G. Z. *J. Phys. Chem. B* **2010**, *114*, 9987−9993.
(40) Wu, B.; Li, C. L.; Yang, H. Y.; Liu, G. M.; Zhang, G. Z. *J. Phys. Chem. B* **2012**, *116*, 3106−3114.
(41) Sun, H. M.; Gao, Z. W.; Yang, L.; Gao, L. X.; Lv, X. S. *Colloid Polym. Sci.* **2010**, *288*, 1713−1722.
(42) Mendrek, B.; Trzebicka, B.; Walach, W.; Dworak, A. *Eur. Polym. J.* **2010**, *46*, 2341−2351.
(43) Rikkou, M. D.; Kolokasi, M.; Matyjaszewski, K.; Patrickios, C. S. *J. Polym. Sci. A: Polym. Chem.* **2010**, *48*, 1878−1886.
(44) Kavitha, A. A.; Singha, N. K. *Macromolecules* **2010**, *43*, 3193−3205.
(45) Li, B. Y.; Shi, Y.; Fu, Z. f.; Yang, W. T.; Jiao, S. K. *Chin. J. Polym. Sci.* **2007**, *25*, 609−619.
(46) Jeon, H. J.; Youk, J. H.; Ahn, S. H.; Choi, J. H.; Cho, K. S. *Macromol. Res.* **2009**, *17*, 240−244.
(47) Naarmann, H.; Hanack, M.; Mattmer, R. *Synthesis* **1994**, *1994*, 477−478.
(48) Krebs, F. C.; Schiødt, N. C.; Batsberg, W.; Bechgaard, K. *Synthesis* **1997**, *1997*, 1285−1290.
(49) Feng, X. S.; Pan, C. Y. *J. Polym. Sci. A: Polym. Chem.* **2001**, *39*, 2233−2243.
(50) Chen, F. G.; Li, C. L.; Wang, X. Y.; Liu, G. M.; Zhang, G. Z. *Soft Matter* **2012**, *8*, 6364−6370.
(51) Rodahl, M.; Höök, F.; Krozer, A.; Brzezinski, P.; Kasemo, B. *Rev. Sci. Instrum.* **1995**, *66*, 3924−3930.
(52) Marin, S. J.; Frye, G. C.; Ricco, A. J.; Senturia, S. D. *Anal. Chem.* **1993**, *65*, 2910−2922.
(53) Sauerbrey, G. *Z. Phys.* **1959**, *155*, 206−222.
(54) Bottom, V. E. *Introduction to Quartz Crystal Unit Design*; Van Nostrand Reinhold: New York, 1982.
(55) Tang, X. D.; Gao, L. C.; Han, N. F.; Fan, X. H.; Zhou, Q. F. *J. Polym. Sci. A: Polym. Chem.* **2007**, *45*, 3342−3348.
(56) Mendrek, B.; Trzebicka, B. *Eur. Polym. J.* **2009**, *45*, 1979−1993.
(57) Gebhardt, J. E.; Fuerstenau, D. W. *Colloids Surf.* **1983**, *7*, 221−231.
(58) Yu, Y. M.; Yin, M. Z.; Müllen, K.; Knoll, W. *J. Mater. Chem.* **2012**, *22*, 7880−7886.
(59) Lee, A. S.; Gast, A. P.; Bütün, V.; Armes, S. P. *Macromolecules* **1999**, *32*, 4302−4310.
(60) Voinova, M. V.; Rodahl, M.; Jonson, M.; Kasemo, B. *Phys. Scr.* **1999**, *59*, 391−396.
(61) Ge, H.; Pispas, S.; Wu, C. *Polym. Chem.* **2011**, *2*, 1071−1076.
(62) Schönhoff, M. *J. Phys.: Condens. Matter* **2003**, *15*, R1781−R1808.
(63) Dobrynin, A. V. *Macromolecules* **2005**, *38*, 9304−9314.
(64) Manning, G. S. *Biophys. J.* **2006**, *91*, 3607−3616.
(65) Gao, Y. Polymolecular and Unimolecular Micelles of Triblock Copolymers. Ph.D. Thesis, Queen's University, Kingston, Ontario, Canada, 2011.
(66) Liu, G. M.; Fu, L.; Rode, A. V.; Craig, V. S. J. *Langmuir* **2011**, *27*, 2595−2600.